Heliyon 10 (2024) e37412

Contents lists available at ScienceDirect

Heliyon

journal homepage: www.cell.com/heliyon

Research article

# Prognostic significance of immune-cell distribution and tumoral spread through air spaces – Multiplex spatial immunophenotyping analysis–

Shunichiro Matsuoka [a,1], Takashi Eguchi [a,*], Mai Iwaya [b,1], Maho Seshimoto [a], Shuji Mishima [a], Daisuke Hara [a], Hirotaka Kumeda [a], Kentaro Miura [a], Kazutoshi Hamanaka [a], Takeshi Uehara [b], Kimihiro Shimizu [a]

[a] Division of General Thoracic Surgery, Shinshu University School of Medicine, Matsumoto, Japan
[b] Department of Laboratory Medicine, Shinshu University School of Medicine, Matsumoto, Japan

ARTICLE INFO

*Keywords:*
Lung cancer
Spread through air spaces
Tumor microenvironment
Immunophenotyping

ABSTRACT

*Objectives:* Spread through air spaces (STAS) is a form of lung cancer invasion that extends beyond the tumor edge and is associated with a worse prognosis. Recent advances in immunotherapy highlight the importance of understanding the tumor microenvironment. This study aimed to investigate the prognostic significance of immune-cell distribution in lung cancer, focusing on the association with STAS.

*Materials and methods:* We retrospectively analyzed 283 patients who underwent curative-intent lung resection for primary lung cancer. Multiplex immunofluorescence staining/phenotyping was performed on tissue microarrays to assess the distribution of CD4, CD8, CD20, CD68, and FoxP3 immune cells within the center and tumor edge. We defined the delta-Edge value (Δ) as the difference in the number of immune cells between the tumor edge and center. Recurrence-free probability (RFP) was analyzed using Kaplan–Meier and Cox proportional hazard models.

*Results:* High ΔCD4 and ΔCD8 values were significantly associated with worse RFP. In stage I adenocarcinoma patients, STAS, and high ΔCD8 were independent risk factors for recurrence. Effect modification analysis revealed that high ΔFoxP3 was significantly associated with worse RFP in patients with STAS, but not in those without STAS. Patients with STAS and high Δimmune cell values had the lowest RFP among all groups.

*Conclusion:* Immune-cell distribution, particularly CD4, CD8, and FoxP3, is a crucial prognostic factor in lung cancer. STAS and specific immune cell distribution patterns can be used to further stratify patient prognosis. Understanding these interactions may provide insights into potential therapeutic targets for personalized lung cancer treatment.

* Corresponding author. Division of General Thoracic Surgery, Department of Surgery, Shinshu University Hospital/Shinshu University School of Medicine 3-1-1 Asahi, Matsumoto, 390-8621, Japan.
*E-mail address:* eguchi_t@shinshu-u.ac.jp (T. Eguchi).
[1] S.M. and M.I. contributed equally to this work.

https://doi.org/10.1016/j.heliyon.2024.e37412
Received 11 September 2023; Received in revised form 2 September 2024; Accepted 3 September 2024
Available online 4 September 2024

## 1. Introduction

Lung cancer remains one of the leading causes of cancer-related deaths worldwide [1]. The high mortality rate associated with lung cancer is primarily attributed to delayed diagnosis in many cases [2]. However, even in patients with early-stage lung cancer undergoing curative-intent lung resection, the risk of recurrence remains significant [3,4]. This highlights the need to effectively identify prognostic factors and improve treatment strategies to better manage this disease.

Recent studies have identified spread through air spaces (STAS) as an independent prognostic factor associated with worse outcomes after lung resection [5]. STAS is a form of tumor invasion whereby tumor cells extend beyond the tumor edge into the surrounding lung parenchyma. Vessel co-option has been proposed as one of the potential mechanisms by which the tumor cells reattach to the alveolar walls [6]. However, the metastatic mechanisms underlying STAS remain unclear, requiring further investigation to elucidate its role in lung cancer progression.

The advent of immunotherapy has revolutionized cancer treatment, offering new therapeutic options for patients with lung cancer [1,7]. However, identifying patients who will benefit from immunotherapy remains challenging, as reliable biomarkers for predicting treatment response are not yet established.

The tumor microenvironment (TME) plays a crucial role in tumor development, progression, and response to therapy [8,9]. The complex interactions between tumor cells and the surrounding TME can modulate tumor aggressiveness, invasion, and metastasis [10]. Among these interactions, the role of immune cells, such as T and B cells, in shaping tumor behavior has garnered considerable attention in recent years.

Given the significance of the TME and the immune response in tumor progression, we hypothesized that the distribution of immune cells (tumor edge vs. center) might be associated with the promotion and prognostic impact of STAS in patients with lung cancer, potentially reflecting a "seed and soil" relationship, with STAS representing the "seed" and immune microenvironment acting as the "soil". This study aimed to investigate the relationship between immune-cell distribution and lung cancer prognosis, focusing on delta-Edge, which is a parameter that reflects the difference in immune cell numbers between the edge and center of a tumor. By analyzing the delta-Edge values of various immune cell subtypes, we aimed to identify potential prognostic factors and gain insights regarding the underlying mechanisms that govern the interaction between tumor cells and the immune response in lung cancer.

## 2. Materials and methods

### 2.1. Patient selection and clinical data

We retrospectively examined 496 consecutive patients who underwent curative-intent lung resection for primary lung cancer between January 2013 and December 2017 at Shinshu University Hospital. We excluded 213 patients diagnosed with lung cancer <1 cm in size, adenocarcinoma *in situ*, minimally invasive adenocarcinoma, neuroendocrine neoplasms, variant histological type, pathological stage IV lung cancer, and analyzed the remaining 283 patients in our study cohort (Fig. 1). This study was approved by the institutional review board of Shinshu University Hospital (project ID: 4723, approved on May 11, 2020).

### 2.2. Tissue microarray construction

Hematoxylin and eosin (H&E) stained slides and paraffin blocks of the tumors in each patient were collected for tissue microarray (TMA) construction. An experienced pathologist (M.I.) evaluated the H&E-stained slides and marked two representative areas in each specimen: the edge and center of the tumor. For the tumor edge, areas were chosen to approximately reflect equal parts of tumor tissue and surrounding lung parenchyma, aiming for a visual estimation of 50 % tumor presence. Subsequently, 3-mm cores of the regions were punched from the paraffin block and inserted into a new paraffin block to develop the TMA (Fig. 2A).

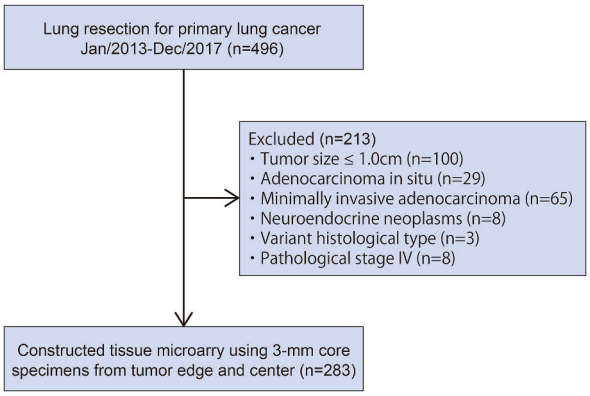


**Fig. 1.** Schema of the study cohort.

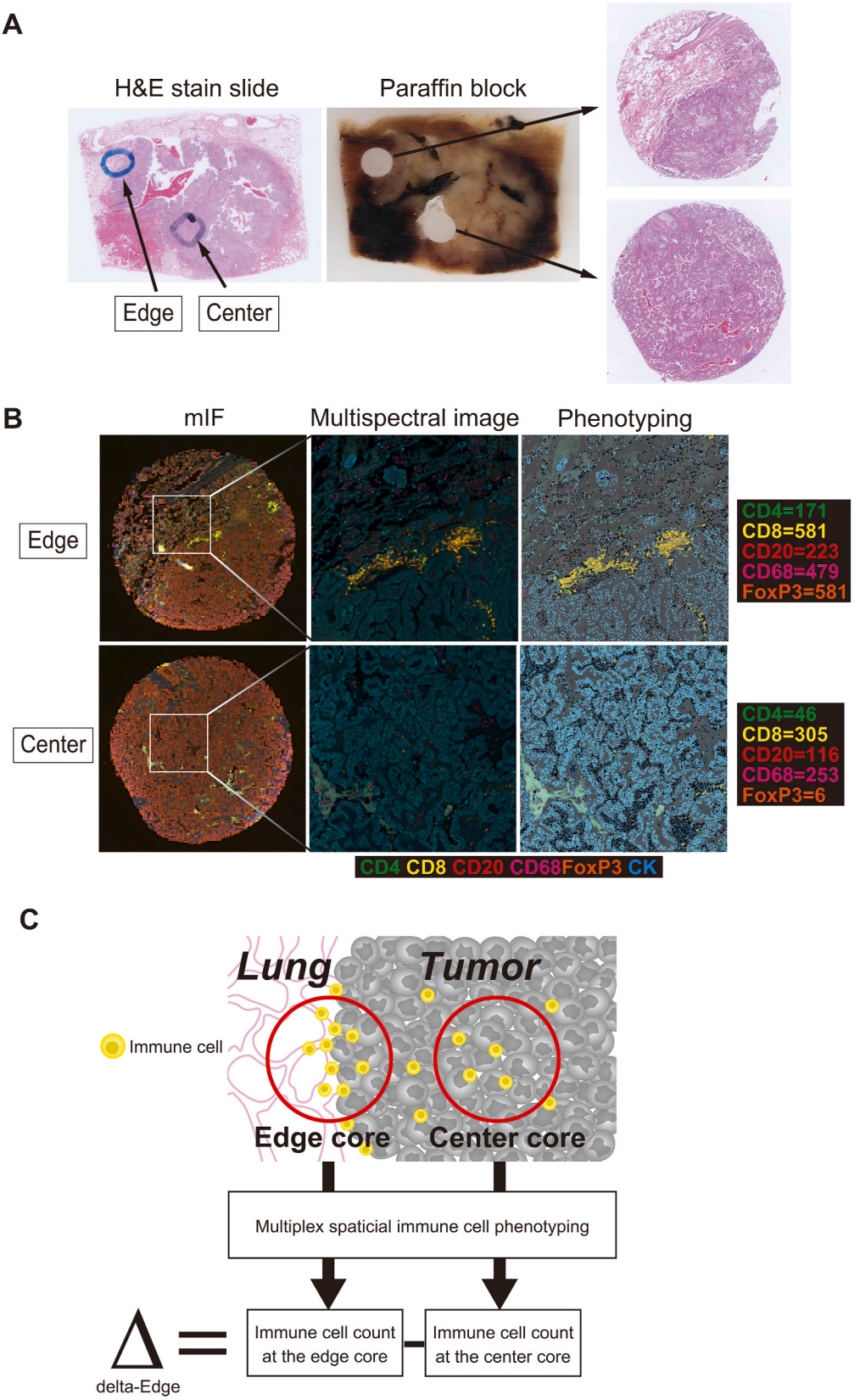


*(caption on next page)*

**Fig. 2.** Pictorial representation of each patient's multiplex spatial immunophenotyping analysis
(A) Tumor edge and center areas were marked on a H&E stained slide, and 3-mm cores of the points were punched from the paraffin block to construct a tissue microarray. (B) mIF staining included CD4, CD8, CD20, CD68, FoxP3, and Pan CK (for tumor cells). Stained slides were imaged using Vectra 3, and individual markers in the multispectral images were quantified through cell segmentation and phenotyping using InForm software. (C) The delta-Edge immune cell value was defined as the difference in the number of immune cells between the tumor edge and center. H&E, hematoxylin and eosin; mIF, multiplex immunofluorescence.

### 2.3. Multiplex immunofluorescence staining

We performed multiplex immunofluorescence (mIF) staining using Opal™ 7 Solid Tumor Immunology Kit (Akoya Biosciences). The mIF panel included CD4 (helper T cells), CD8 (cytotoxic T cells), CD20 (B cells), CD68 (macrophages), FoxP3 (regulatory T cells), Pan-CK (tumor cells), and 4′,6-diamidino-2-phenylin-dole (DAPI, nuclear staining). Four micrometer sections obtained from TMA blocks were deparaffinized with xylene and ethanol solutions, and antigen retrieval was performed using microwave treatment. After blocking, the sections were subjected to six sequential rounds of staining, including each primary antibody incubation, microwave treatment, horseradish peroxidase, and fluorophore labeling, followed by a final cycle of DAPI staining and slide mounting.

### 2.4. Image acquisition and cell phenotyping

The stained slides were imaged using Vectra 3 quantitative pathology imaging system (Akoya Biosciences). After a whole slide scan at low magnification (4 × ), each core was captured as a multispectral image at a higher resolution (20 × ). The image files were analyzed using InForm software (Akoya Biosciences), and the individual markers were characterized and quantified through cell segmentation and cell phenotyping (Fig. 2B).

### 2.5. Definition of delta-Edge value

To investigate the immune-cell distribution of lung cancer, we defined delta-Edge as the difference in the number of immune cells between the tumor edge and center (Fig. 2C). In short, a high delta-Edge value represents a larger number of immune cells at the tumor edge than at the center.

### 2.6. The formula for calculating the delta-Edge value of immune cells

Δ (Delta) [immune cell] = {number of [immune cell] at the tumor edge core} - {number of [immune cell] at the tumor center core}

**Table 1**
Demographics of all patients and comparison with and without spread through air spaces.

| Characterisitc | | STAS | | | | | | |
|---|---|---|---|---|---|---|---|---|
| | | All cases (n = 283) | | Negative (n = 166) (59 %)* | | Positive (n = 117) (41 %)* | | *P* value |
| Age | | 70 | (63–75) | 71 | (65–75) | 69 | (62–73) | **0.032** |
| Gender | Male | 159 | (56) | 97 | (58) | 62 | (53) | 0.364 |
| | Female | 124 | (44) | 69 | (42) | 55 | (47) | |
| Surgery | Wedge resection | 20 | (7) | 14 | (8) | 6 | (5) | 0.559 |
| | Segmentectomy | 10 | (4) | 6 | (4) | 4 | (3) | |
| | Lobectomy | 253 | (89) | 146 | (88) | 107 | (91) | |
| Histology | Ad | 221 | (78) | 117 | (70) | 104 | (89) | **<0.001** |
| | SCC | 62 | (22) | 49 | (30) | 13 | (11) | |
| Pathological tumor size | | 2 | (2–4) | 2 | (2–4) | 3 | (2–3) | 0.589 |
| Pathological invasive size | | 2 | (2–3) | 2 | (1–3) | 2 | (2–3) | 0.502 |
| Pleural invasion | Positive | 68 | (24) | 37 | (13.1) | 31 | (26.5) | 0.415 |
| Lyphatic invasion | Positive | 62 | (22) | 24 | (15) | 38 | (33) | **<0.001** |
| Vascular invasion | Positive | 81 | (29) | 44 | (27) | 37 | (32) | 0.348 |
| Lymphovascular invasion | Positive | 37 | (13) | 15 | (9) | 22 | (19) | **0.016** |
| Pathological stage | I | 197 | (70) | 124 | (75) | 73 | (62) | 0.057 |
| | II | 47 | (17) | 25 | (15) | 22 | (19) | |
| | III | 39 | (14) | 17 | (10) | 22 | (19) | |
| Delta-Edge immune cell† | ΔCD4 | 14 | (-101; 140) | 9 | (-189; 128) | 18 | (-36; 195) | 0.178 |
| | ΔCD8 | −23 | (-506; 158) | −26 | (-574; 117) | −6 | (-355; 224) | 0.134 |
| | ΔCD20 | −1 | (-91; 38) | −3 | (-95; 48) | 0 | (-88; 29) | 0.939 |
| | ΔCD68 | 102 | (-3; 261) | 76 | (-44; 222) | 146 | (29; 292) | **0.005** |
| | ΔFoxp3 | 5 | (-10; 31) | 5 | (-13; 27) | 6 | (-8; 36) | 0.364 |

Values are presented as n (%) or median (25th-75th or 25th; 75th percentile). Ad, adenocarcinoma; SCC, squamous cell carcinoma; STAS, spread through air paces. *Percentages in parentheses indicate the proportion of patients who have STAS or no STAS, respectively. †Delta-Edge immune = edge - center immune cell in each tumor.

### 2.7. Statistical analysis

Patient clinicopathologic data are presented as the number (percentage) or median (interquartile range) and compared using the chi-square test for categorical variables and the Mann–Whitney *U* test for continuous variables between two groups. Recurrence-free probability (RFP) was estimated using the Kaplan–Meier method and compared between groups by the log-rank test. Cox proportional hazard analysis was performed to determine risk factors for RFP. Multivariable analysis was performed using a backward selection approach with $P \leq 0.2$ obtained from the univariable analyses. We performed all statistical analyses using IBM SPSS Statistics version 27 software (IBM, Armonk, NY, USA), and statistical significance was set at $P < 0.05$.

## 3. Results

### 3.1. Association between delta-Edge of immune cells and recurrence

Table 1 presents the clinicopathologic demographics of 283 patients and compares patients with and without STAS. The median age was 70 years, and 159 (56 %) patients were men. Among the 283 patients, 253 (89 %) underwent lobectomy, 10 (4 %) underwent segmentectomy, and 20 (7 %) underwent wedge resection. Most patients had adenocarcinoma (78 %) and pathological stage I disease (70 %). The median follow-up period was 58 months. Of the total patients, STAS was observed in 117 patients (41 %). The presence of STAS was significantly associated with lower age ($p = 0.032$), adenocarcinoma ($p < 0.001$), and higher ΔCD68 ($p = 0.005$).

Fig. 3A–E demonstrates the association between RFP and Δimmune cells. Patients with high ΔCD4 had significantly worse RPF (5-year RFP, 64 %) than those with low ΔCD4 (5-year RFP, 74 %; $p = 0.028$) (Fig. 3A). Similarly, there was a significant difference between patients with high and low ΔCD8 (5-year RFP, 61 % vs. 78 %; $p < 0.001$) (Fig. 3B). There was a trend toward worse RFP in patients with high ΔCD20, but no significant differences between ΔCD20, ΔCD68, and ΔFoxP3 groups (Fig. 3C–E).

The prognosis of stage I patients was also shown according to Δimmune cells in Fig. 4. The RFP was significantly worse for stage I patients with high ΔCD4 and ΔCD8 compared to low ΔCD4 and ΔCD8, respectively (5y-RFP of ΔCD4, 76 % vs. 86 %, $p = 0.048$; 5y-RFP of ΔCD8, 75 % vs. 89 %; $p < 0.001$).

### 3.2. Association between delta-Edge of immune cells and adenocarcinoma subtypes in stage I patients

Table 2 presents the clinicopathologic demographics of 162 patients with stage I adenocarcinoma. The most common subtype was acinar predominant adenocarcinoma (33.4 %), followed by papillary predominant (32.6 %), lepidic predominant (LPA) (17 %), solid predominant (SPA) (11 %), and micropapillary predominant (1 %). Fig. 5 illustrates significant differences in Δimmune cells across

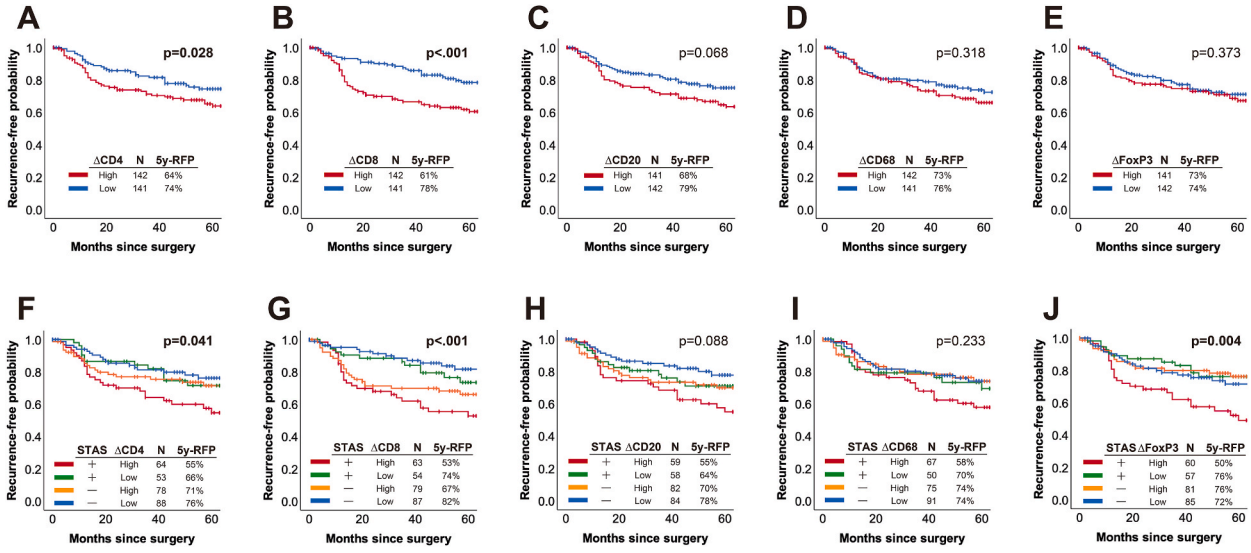


**Fig. 3.** Kaplan–Meier curves of recurrence-free probability (RFP) according to Δimmune cell status (A–E) and between four groups based on the combination of spread through air spaces (STAS) and each Δimmune cell value (F-J)
The RFP of patients with high ΔCD4 (A) and ΔCD8 (B) were significantly worse than those with low ΔCD4 and ΔCD8, respectively (5-year RFP of ΔCD4, 64 % vs. 74 %, $p = 0.028$; 5-year RFP of ΔCD8, 61 % vs. 78 %; $p < 0.001$). There were no differences for ΔCD20, ΔCD68, and ΔFoxP3 status (C, D, and E). Patients with STAS and high Δ CD4 (F), ΔCD8 (G), and ΔFoxP3 (J) had the significantly worst RFP among the four groups, respectively (5y-RFP of ΔCD4, 55 %, $p = 0.041$; 5y-RFP of ΔCD8, 53 %, $p < 0.001$; 5y-RFP of ΔFoxP3, 50 %, $p = 0.004$).

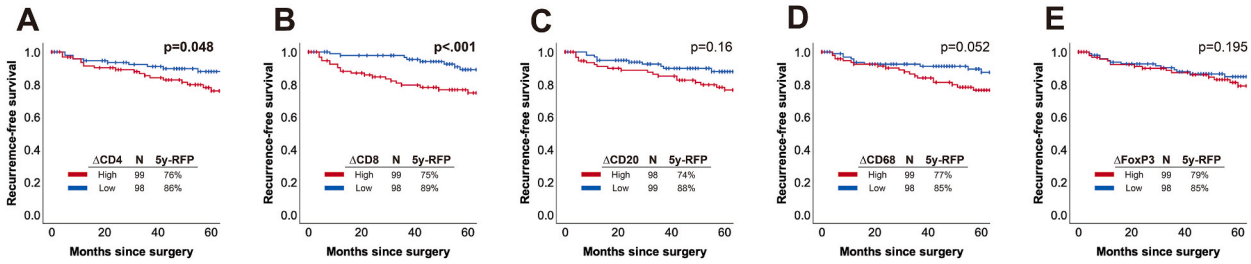


**Fig. 4.** Kaplan–Meier curves of recurrence-free probability (RFP) of stage I patients according to Δimmune cell status
The RFP of stage I patients with high ΔCD4 (A) and ΔCD8 (B) were significantly worse than those with low ΔCD4 and ΔCD8, respectively (5-year RFP of ΔCD4, 76 % vs. 86 %, p = 0.048; 5-year RFP of ΔCD8, 75 % vs. 89 %; p < 0.001). There were no differences for ΔCD20, ΔCD68, and ΔFoxP3 status (C, D, and E).

**Table 2**
Demographics of stage I adenocarcinoma patients and comparison with and without spread through air spaces.

| | | | | STAS | | | | |
|---|---|---|---|---|---|---|---|---|
| Characterisitc | | All cases (n = 162) | | Negative (n = 95) (59 %)* | | Positive (n = 67) (41 %)* | | *P* value |
| Age | | 68 | (62–74) | 95 | (62–75) | 68 | (63–73) | 0.346 |
| Gender | Male | 72 | (44) | 41 | (43) | 31 | (46) | 0.695 |
| | Female | 90 | (56) | 54 | (57) | 36 | (54) | |
| Surgery | Wedge resection | 11 | (7) | 9 | (10) | 2 | (3) | 0.257 |
| | Segmentectomy | 8 | (5) | 5 | (5) | 3 | (5) | |
| | Lobectomy | 143 | (88) | 81 | (85) | 62 | (92) | |
| Pathological tumor size | | 2 | (1.5–2.7) | 1.9 | (1.5–2.5) | 2.2 | (1.6–3.2) | 0.138 |
| Pathological invasive size | | 1.6 | (1.2–2.2) | 1.6 | (1.2–2) | 1.8 | (1.2–2.4) | 0.116 |
| Pleural invasion | Positive | 23 | (14) | 8 | (8) | 15 | (22) | **0.012** |
| Lymphatic invasion | Positive | 14 | (9) | 4 | (4) | 10 | (15) | **0.017** |
| Vascular invasion | Positive | 21 | (13) | 10 | (11) | 11 | (16) | 0.272 |
| Tumor grade | 1–2 | 121 | (75) | 78 | (82) | 43 | (64) | **0.007** |
| | 3 | 41 | (25) | 17 | (18) | 24 | (36) | |
| Predominant subtype | Lepidic | 28 | (17) | 20 | (21) | 8 | (12) | **0.032** |
| | Acinar | 54 | (34) | 31 | (33) | 23 | (34) | |
| | Papillary | 53 | (32) | 29 | (31) | 24 | (36) | |
| | Microapillary | 1 | (1) | 0 | (0) | 1 | (2) | |
| | Solid | 18 | (11) | 7 | (7) | 11 | (16) | |
| | Others | 8 | (5) | 8 | (8) | 0 | (0) | |
| Delta-Edge immune cell† | ΔCD4 | 4 | (-302; 149) | −5 | (-364; 156) | 13 | (-230; 118) | 0.307 |
| | ΔCD8 | −95 | (-692; 45.5) | −126 | (-897; 17) | −76 | (-542; 168) | 0.088 |
| | ΔCD20 | −4 | (-106; 32) | −5 | (-94; 39) | −3 | (-136; 28) | 0.84 |
| | ΔCD68 | 112 | (-7; 264) | 70 | (-58; 216) | 159 | (30; 292) | **0.007** |
| | ΔFoxp3 | 4 | (-23; 29) | 4 | (-26; 24) | 3 | (-10; 33) | 0.431 |

Values are presented as n (%) or median (25th-75th or 25th; 75th percentile). STAS, spread through air paces. *Percentages in parentheses indicate the proportion of patients who have STAS or no STAS, respectively. †Delta-Edge immune = edge - center immune cell in each tumor.

these subtypes, notably in ΔCD4 and ΔCD8 levels (ΔCD4, p = 0.024; ΔCD8, p < 0.001) as detailed in Fig. 5A and B.

Fig. 5F–I provide a detailed breakdown of each Δimmune cell value across adenocarcinoma subtypes, further illustrating these relationships. In LPA, which is known to be associated with a better prognosis, Δ values across all immune cells were lower compared to other subtypes. Notably, ΔCD8 was the lowest in LPA, with 78 % of patients exhibiting low ΔCD8 levels (Fig. 5F). This suggests a less pronounced immune response in this subtype. Conversely, in SPA, which is associated with a worse prognosis, Δ values across all immune cells were higher compared to other subtypes. Among these, ΔCD8 was the highest, with 94 % of SPA patients exhibiting high ΔCD8 levels (Fig. 5I). This indicates a markedly stronger immune response in SPA, which may reflect an evolved mechanism for immune evasion or a more aggressive disease phenotype.

This contrasting relationship between LPA and SPA subtypes is particularly interesting. While LPA patients tend to have low Δ values in immune cells, indicative of a more subdued immune environment, SPA patients show elevated Δ values, especially in ΔCD8, suggesting a complex interaction between immune activity and tumor aggressiveness. These findings underscore the importance of considering immune profiles in understanding the prognosis of different adenocarcinoma subtypes.

### *3.3. Multivariable analysis for recurrence in stage I adenocarcinoma patients*

We performed Cox hazard model analysis to evaluate prognostic impact of Δ values of immune cells incorporating critical histologic factors such as histologic subtypes, tumor grade, lymphatic invasion, vascular invasion, and pleural invasion, recognizing their

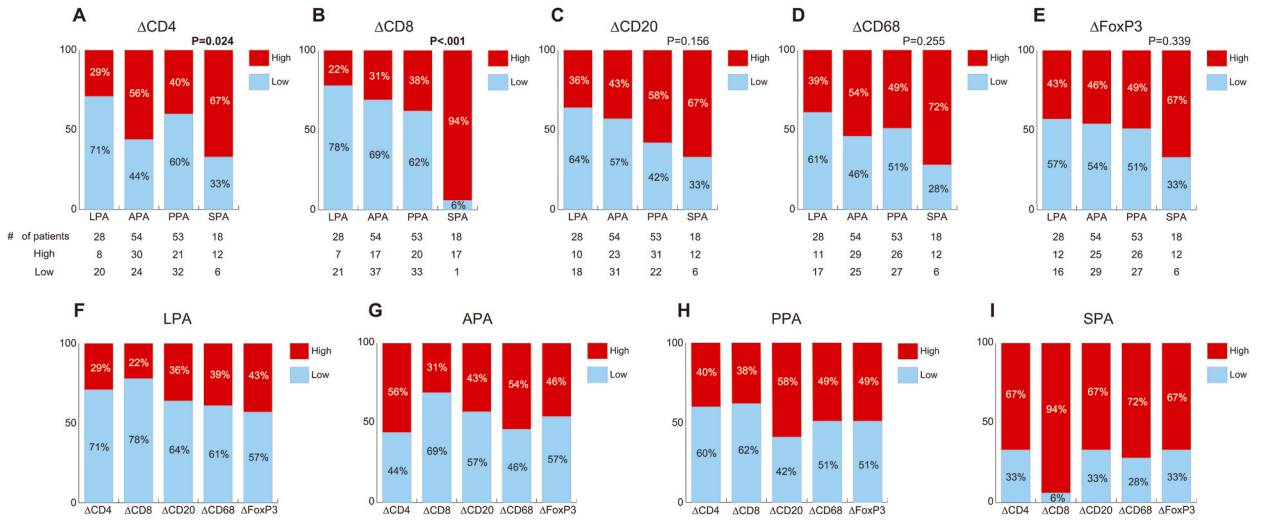


**Fig. 5.** The association between adenocarcinoma subtypes and each Δimmune cell value in stage I patients
There were significant differences in ΔCD4 and ΔCD8 across adenocarcinoma subtypes, respectively (ΔCD4, p = 0.024; ΔCD8, p < 0.001) (A and B). ΔCD8 was the lowest in LPA, with 78 % of patients exhibiting low ΔCD8 levels (F). Conversely, ΔCD8 was the highest, with 94 % of SPA patients exhibiting high ΔCD8 levels (I). Micropapillary predominant adenocarcinoma was not included in this analysis because of the small sample size (n = 1).
LPA, lepidic predominant adenocarcinoma; APA, acinar predominant adenocarcinoma; PPA, papillary predominant adenocarcinoma; SPA, solid predominant adenocarcinoma.

importance in lung cancer prognosis, particularly in stage I adenocarcinoma. Initially, we examined the associations between STAS and these additional histologic variables, as detailed in Table 2. This preliminary analysis revealed significant associations of STAS with higher tumor grade, lymphatic invasion, and pleural invasion, highlighting their relevance in the context of recurrence risk.In response

**Table 3**
Cox proportional hazard analysis for recurrence-free probability in stage I adenocarcinoma patients.

| | | Univariable | | | Multivariable backward stepwise LR* | | | | | |
|---|---|---|---|---|---|---|---|---|---|---|
| | | | | | Initial step | | | Final step | | |
| **Characterisitc** | | **HR** | **(95%CI)** | ***P* value** | **HR** | **(95%CI)** | ***P* value** | **HR** | **(95%CI)** | ***P* value** |
| Age | (per 1 year increase) | 1.03 | (0.98–1.08) | 0.28 | | | | | | |
| Gender Female | (vs Male) | 0.60 | (0.27–1.38) | 0.23 | | | | | | |
| Surgery | Wedge resection (Ref) | 1 | | 0.66 | | | | | | |
| | Segmentectomy | 0.47 | (0.04–5.14) | | | | | | | |
| | Lobectomy | 0.52 | (0.12–2.21) | | | | | | | |
| Pathological tumor size | (per 1 cm increase) | 1.17 | (0.86–1.58) | 0.331 | | | | | | |
| Pathological invasive size | (per 1 cm increase) | 1.55 | (0.95–2.53) | **0.078** | 1.35 | (0.74–2.46) | 0.335 | | | |
| Predominant subtype | Lepidic (Ref) | 1.00 | | **0.01** | 1.00 | | 0.342 | | | |
| | Acinar | 0.67 | (0.18–2.51) | | 0.29 | (0.07–1.33) | | | | |
| | Papillary | 0.62 | (0.17–2.31) | | 0.30 | (0.06–1.39) | | | | |
| | Micropapillary | | NA | | | NA | | | | |
| | Solid | 3.99 | (1.20–13.23) | | 1.57 | (0.27–9.16) | | | | |
| | Others | 1.37 | (0.15–12.32) | | 0.82 | (0.06–10.63) | | | | |
| Tumor grade | 1-2 (Ref) | 1.00 | | **<0.001** | 1.00 | | 0.879 | | | |
| | 3 | 4.60 | (2.01–10.52) | | 1.12 | (0.27–4.56) | | | | |
| Pleural invasion | (vs Negative) | 8.31 | (3.66–18.86) | **<0.001** | 8.93 | (2.63–30.33) | **<0.001** | 8.26 | (3.57–19.12) | **<0.001** |
| Lymphatic invasion | (vs Negative) | 2.88 | (0.98–8.49) | **0.055** | 3.01 | (0.68–13.3) | 0.147 | | | |
| Vascular invasion | (vs Negative) | 3.07 | (1.26–7.47) | **0.013** | 0.26 | (0.06–1.08) | 0.063 | | | |
| STAS | (vs Negative) | 2.69 | (1.14–6.34) | **0.024** | 1.03 | (0.33–3.22) | 0.957 | | | |
| High ΔCD4 | (vs Low) | 2.59 | (1.06–6.29) | **0.036** | 1.55 | (0.51–4.73) | 0.444 | | | |
| High ΔCD8 | (vs Low) | 2.51 | (1.03–6.10) | **0.043** | 2.97 | (0.97–9.04) | 0.056 | 3.31 | (1.36–8.09) | **0.009** |
| High ΔCD20 | (vs Low) | 2.59 | (1.07–6.31) | **0.036** | 1.11 | (0.37–3.35) | 0.853 | | | |
| High ΔCD68 | (vs Low) | 2.40 | (0.99–5.82) | **0.054** | 0.84 | (0.28–2.50) | 0.752 | | | |
| High ΔFoxP3 | (vs Low) | 1.93 | (0.82–4.55) | **0.13** | 1.63 | (0.62–4.32) | 0.325 | | | |

HR, hazard ratio; CI, confidence interval; STAS, spread through air paces; NA, not applicable.*Multivariable analysis included the variables that had a P value of <0.2 in univariable analysis.

to these findings, we conducted a comprehensive multivariate Cox regression analysis to assess the risk of recurrence. This analysis incorporated all variables with a p-value <0.2 from the univariable analyses. The results, summarized in Table 3, identified pleural invasion and high ΔCD8 levels as independent prognostic factors. Additionally, to address potential issues of overfitting and collinearity, which could compromise the interpretability and robustness of our findings, we performed additional separate analyses for each group of variables. These analyses are detailed in Supplemental Tables S1–S5.

### 3.4. Impact of FoxP3+ regulatory T-cell infiltration on STAS-associated prognosis

We performed an effect modification analysis to examine the potential interaction between the presence of STAS and the distribution of immune cells in the TME. This analysis aimed to uncover whether the combination of STAS and specific immune cell distribution patterns could further stratify the prognostic implications for patients with lung cancer.

Fig. 3F–J shows a comparison between four groups based on the combination of STAS and each Δimmune cell value; patients with STAS who had high Δimmune, with STAS and low Δimmune, without STAS and high Δimmune, and without STAS and low Δimmune. In all immune cells, patients with STAS and high Δimmune cell values had the lowest RFP. In CD4, CD8, and FoxP3 analyses, there were statistically significant prognostic differences among the four groups (Fig. 3F, G, and J).

The Kaplan–Meier curves illustrate the association between RFP and the combination of STAS and immune cell distribution (Figs. 6 and 7). In patients with STAS, high ΔCD8 was associated with significantly worse RFP (5-year RFP, 44 %) than those with low ΔCD8 (5-year RFP, 74 %; p = 0.008) (Fig. 6A). A similar result was observed in patients without STAS regarding high and low ΔCD8 values (5-year RFP, 61 % vs. 82 %; p = 0.046) (Fig. 6B). However, high ΔFoxP3 was significantly associated with worse RFP (5-year RFP, 41 %) than low ΔFoxP3 in patients with STAS (5-year RFP, 76 %; p = 0.022) (Fig. 6C), while no difference was found between high and low ΔFoxP3 in those without STAS (5-year RFP, 72 % vs. 66 %; p = 0.43) (Fig. 6D). There were no differences between high and low Δimmune cell values in ΔCD4, ΔCD20, and ΔCD68 groups (Fig. 7).

## 4. Discussion

Our study provides valuable insights into the role of immune-cell distribution in lung cancer aggressiveness and prognosis. The strength and novelty of this study are as follows: 1) we are the first to develop a TMA that evaluates both tumor center and edge with a specific focus on immune-cell distribution and STAS; 2) we defined delta-Edge and evaluated immune-cell distribution using a multiplex platform, discovering that immune-cell penetration by anti-tumor immune cells, such as $CD8^+$ T cells, was associated with patient prognosis; 3) we found that the presence of FoxP3+ regulatory T cells in the tumor edge was only associated with worse prognosis in patients with STAS, suggesting a mechanistic link between pro-tumor immune cells, STAS, and tumor aggressiveness. These findings highlight the importance of understanding the complex interplay between tumor cells and the surrounding immune cells within the TME.

A key finding of our study is that tumors that protect themselves from anti-tumor immune-cell infiltration are associated with worse prognosis, regardless of pathological prognosticators, such as STAS. This observation suggests that the inability of immune cells to penetrate the tumor's core enables tumor survival and progression. This novel finding highlights the significance of the spatial distribution of immune cells in the TME. It underscores the need to consider immune cell localization when evaluating the immunological landscape of lung cancer.

Our study also revealed that higher delta-Edge values of $CD8^+$ T cells, known as cytotoxic T cells, were strongly associated with worse prognosis even in patients with early-stage lung cancer who underwent curative-intent resection. This finding emphasizes the importance of considering immunotherapy as an adjuvant therapy to prevent recurrence in patients with early-stage lung cancer. It also suggests the need to investigate the TME with a focus on immune-cell distribution in patients undergoing adjuvant

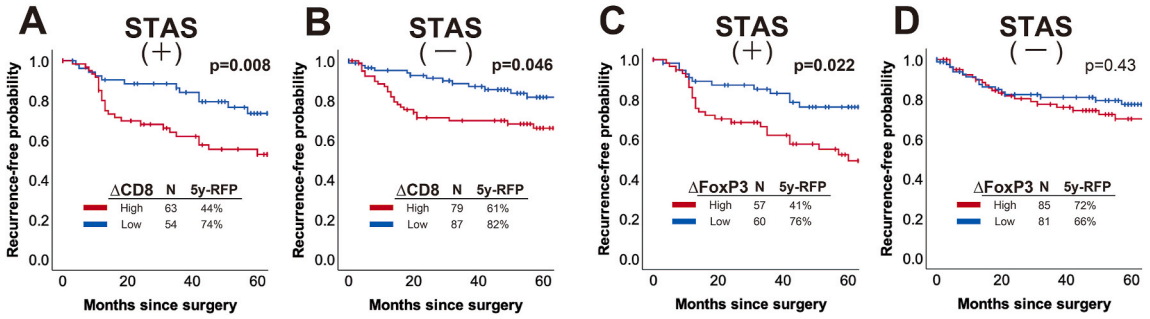


**Fig. 6.** Kaplan–Meier curves of recurrence-free probability (RFP) of each Δimmune cell (CD8, and FoxP3) according to spread through air spaces (STAS) status

Patients with high ΔCD8 had worse RFP in both STAS-positive and STAS-negative groups compared to those with low ΔCD8 (5-year RFP low ΔCD8 vs. high ΔCD8 in STAS-positive, 74 % vs. 44 %, p = 0.008; in STAS-negative, 82 % vs. 61 %, p = 0.046) (A and B).

High ΔFoxP3 was significantly associated with worse RFP than low ΔFoxP3 only in patients with STAS, but not in those without STAS (5-year RFP low ΔFoxP3 vs. high ΔFoxP3 in STAS-positive, 76 % vs. 41 %, p = 0.022; in STAS-negative, 66 % vs. 72 %, p = 0.430) (C and D).

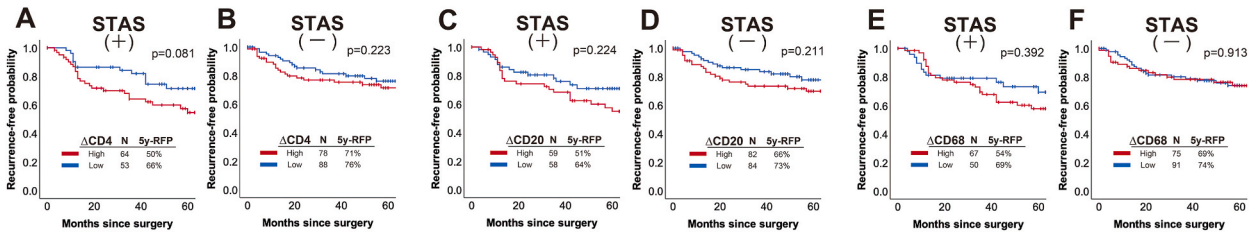


**Fig. 7.** Kaplan–Meier curves of recurrence-free probability (RFP) of each Δimmune cell (CD4, CD20, and CD68) according to spread through air spaces (STAS) status
There were no differences between high and low Δimmune cell values in ΔCD4, ΔCD20, and ΔCD68 groups.

immunotherapy to better understand the relationship between the treatment effect and immune-cell distribution. This approach could help tailor individualized immunotherapy strategies for patients and potentially improve patient outcomes.

Adenocarcinoma subtypes exhibit varied prognoses and immune profiles, which could significantly influence patient outcomes and immune cell distribution. To address this, we performed a detailed analysis of immune cell Δ-edge values across different adenocarcinoma subtypes. Our findings indicate substantial differences in the immune response, notably in ΔCD4 and ΔCD8 levels across these subtypes. For instance, patients with SPA exhibited significantly higher ΔCD8 levels (94 %) compared to other subtypes: lepidic (22 %), acinar (31 %), and papillary (38 %) with a statistically significant p-value of less than 0.001. This suggests that SPA, associated with a more robust immune response, might also correlate with distinct clinical behaviors, potentially indicating a more aggressive disease phenotype with an evolved mechanism for evading immune surveillance.

Understanding how tumors protect themselves from anti-tumor immune-cell infiltration is critical for developing new therapeutic approaches to modify or overcome these mechanisms. Future research should focus on elucidating the complex interactions and molecular pathways that enable tumors to evade immune surveillance and resist infiltration by anti-tumor immune cells. Identifying key mediators of these processes could lead to the development of novel therapies that can effectively overcome these protective mechanisms and boost the immune response against lung cancer.

Another pivotal finding from our study is the intricate relationship between the presence of FoxP3+ regulatory T cells at the tumor edge and poorer prognosis in patients with STAS-positive tumors. FoxP3+ T cells are generally recognized for their immunosuppressive role, which traditionally is thought to facilitate tumor progression by dampening effective anti-tumor immune responses. In our analysis, while FoxP3+ cells themselves were not independent predictors of RFP, the presence of STAS emerged as a significant independent risk factor. This differential impact underscores a crucial observation: in the context of STAS, FoxP3+ T cells at the tumor margin appear to enhance tumor invasiveness. This suggests that these regulatory T cells contribute to a microenvironment that supports tumor cell migration and invasion, particularly when coupled with the structural disruptions characteristic of STAS. Therefore, the interaction between FoxP3+ cells and STAS may potentiate the spread of tumor cells into adjacent lung tissues, markedly worsening the prognosis. This dynamic aligns with the 'seed and soil' theory of metastasis, where the 'seed' (the tumor cells facilitated by STAS) finds a conducive 'soil' (an immune environment modulated by FoxP3+ cells) that enhances its invasive potential. Our findings provide a novel mechanistic insight into how the distribution of specific immune cells within the tumor microenvironment, particularly at the invasive front, can significantly influence cancer progression and patient outcomes. (Fig. 8).

Our study results have several clinical implications. By understanding the effect of immune-cell distribution on lung cancer aggressiveness and prognosis, clinicians can better stratify patients according to their risk of recurrence and guide treatment decisions. Additionally, our findings may encourage the exploration of combination therapies that simultaneously target tumor cells (STAS "seeds") and the immunosuppressive TME ("soil"), thus providing a more comprehensive approach to combat lung cancer.

Although our study offers novel insights into the role of immune-cell distribution in lung cancer prognosis, some limitations should be considered. First, the study is retrospective, and therefore, the findings may be influenced by potential biases and confounding factors. Second, while TMA facilitates efficient comparative analysis across multiple samples, it does not capture the full spatial and histological heterogeneity of tumors as comprehensively as full-section examinations. This limitation may affect the accurate representation and interpretation of immune cell distributions and their spatial dynamics within the tumor microenvironment. Additionally, our use of mIF staining, although effective for detailed cellular phenotyping, was confined to a specific set of biomarkers. This approach might not fully capture the diverse functional states and complexities of immune cells involved in tumor dynamics. We acknowledge these methodological constraints and are planning more extensive studies that will employ a broader spectrum of biomarkers and involve larger sample sizes. These future investigations aim to enhance our understanding of the nuanced interactions between immune cell distributions, STAS, and their implications for lung cancer prognosis. The insights from these studies are expected to inform more precise therapeutic targeting of immune pathways in oncology. Third, the scope of immune cells analyzed in this study was limited; we did not assess several cell types integral to the tumor microenvironment such as fibroblasts, myeloid-derived suppressor cells, and M2 macrophages. Additionally, we did not evaluate the expression of several key immunological markers including programmed cell death-1 and its ligand, cytotoxic T-lymphocyte-associated protein 4, and lymphocyte activation gene-3. These components are critical for understanding the interplay between immune-cell distribution and immunotherapy responses. Future research will need to address these gaps to provide a more comprehensive picture of the tumor immune landscape and its impact on therapy efficacy. Fourth, the sample size is relatively small, particularly for micropapillary and solid predominant adenocarcinoma. Therefore, this study does not exclude the possibility that these aggressive subtypes instead of STAS may influence

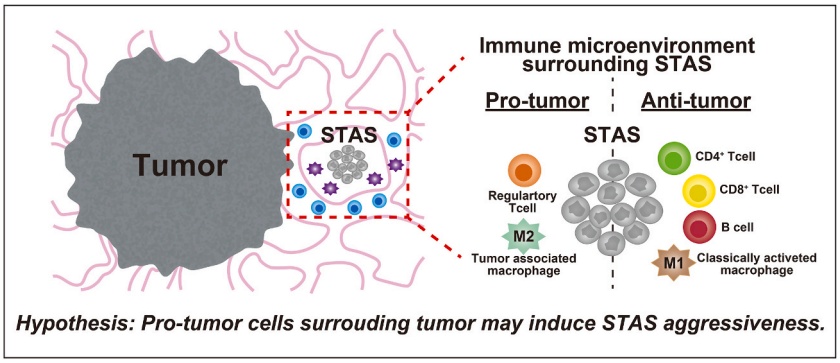


**Fig. 8.** Schema of immune microenvironment surrounding spread through air spaces (STAS)
Pro-tumor cells at the tumor edge may induce STAS aggressiveness.

the immune cells. Larger, prospective studies are required to validate our findings and further explore the complex relationship between immune-cell distribution, STAS, and lung cancer prognosis. Fifth, our methodology for marking the tumor edge involved an estimation rather than a precise measurement of the ratio of tumor tissue to lung parenchyma. This could potentially affect the distribution of immune cells measured in our study. Future investigations will incorporate digital imaging and quantitative analyses to accurately determine and control these tissue ratios, thereby reducing variability and enhancing the reliability of our immune cell data.

## 5. Conclusion

Our study highlights the importance of immune-cell distribution in determining lung cancer aggressiveness and prognosis. Our findings emphasize the potential therapeutic value of targeting immune cells, particularly FoxP3+ regulatory T cells, and modulating the TME with a focus on anti-tumor immune cell penetration, to improve patient outcomes. Further investigation into the underlying mechanisms and the development of innovative therapeutic approaches will be crucial for translating these findings into clinical practice and ultimately improving the management and outcomes of patients with lung cancer.

## Funding

This study was supported by the Grant-in-Aid for Early-Career Scientists from the Japan Society for the Promotion of Science (No. 20K17742).

## Disclosure statement

The authors have no conflict of interest to be declared.

## Ethics declarations

This study was approved by the Institutional Review Board of Shinshu University Hospital (project ID: 4723, approved on May 11, 2020). An opt-out approach was utilized in lieu of obtaining written informed consent.

## Data availability statement

Due to ethical restrictions, supporting data for this study cannot be provided.

## CRediT authorship contribution statement

**Shunichiro Matsuoka:** Writing – review & editing, Writing – original draft, Methodology, Investigation, Formal analysis, Data curation, Conceptualization. **Takashi Eguchi:** Writing – review & editing, Writing – original draft, Methodology, Investigation, Formal analysis, Data curation, Conceptualization. **Mai Iwaya:** Writing – review & editing, Methodology, Investigation. **Maho Seshimoto:** Writing – review & editing. **Shuji Mishima:** Writing – review & editing. **Daisuke Hara:** Writing – review & editing. **Hirotaka Kumeda:** Writing – review & editing. **Kentaro Miura:** Writing – review & editing. **Kazutoshi Hamanaka:** Writing – review & editing. **Takeshi Uehara:** Writing – review & editing. **Kimihiro Shimizu:** Writing – review & editing.

## Declaration of generative AI and AI-assisted technologies in the writing process

None declared.

## Declaration of competing interest

None declared.

## Acknowledgments

We would like to thank S. Shimoeda and M. Nomura for their support with immunofluorescent staining. We would also like to thank Editage (www.editage.com) for the English language editing.

## Appendix A. Supplementary data

Supplementary data to this article can be found online at https://doi.org/10.1016/j.heliyon.2024.e37412.

## References

[1] A.A. Thai, B.J. Solomon, L.V. Sequist, J.F. Gainor, R.S. Heist, Lung cancer, Lancet 398 (2021) 535–554, https://doi.org/10.1016/s0140-6736(21)00312-3.
[2] R.L. Siegel, M.D. Miller, H.E. Fuchs, A. Jemal, Cancer Statistics, CA Cancer J. Clin. 71 (2021) 7–33, https://doi.org/10.3322/caac.21654, 2021.
[3] B.T. Heiden, D.B. Eaton Jr., K.E. Engelhardt, S. Chang, Y. Yan, M.R. Patel, D. Kreisel, R.G. Nava, B.F. Meyers, B.D. Kozower, V. Puri, Analysis of delayed surgical treatment and oncologic outcomes in clinical stage I non-small cell lung cancer, JAMA Netw. Open 4 (2021) e2111613, https://doi.org/10.1001/jamanetworkopen.2021.11613.
[4] W.G. Jeong, H. Choi, K.J. Chae, J. Kim, Prognosis and recurrence patterns in patients with early stage lung cancer: a multi-state model approach, Transl, Lung Cancer Res 11 (2022) 1279–1291, https://doi.org/10.21037/tlcr-22-148.
[5] T. Eguchi, K. Kameda, S. Lu, M.J. Bott, K.S. Tan, J. Montecalvo, J.C. Chang, N. Rekhtman, D.R. Jones, W.D. Travis, P.S. Adusumilli, Lobectomy is associated with better outcomes than sublobar resection in spread through air spaces (STAS)-positive T1 lung adenocarcinoma: a propensity score-matched analysis, J. Thorac. Oncol. 14 (2019) 87–98, https://doi.org/10.1016/j.jtho.2018.09.005.
[6] Y. Yagi, R.G. Aly, K. Tabata, A. Barlas, N. Rekhtman, T. Eguchi, J. Montecalvo, M. Hameed, K. Manova-Todorova, P.S. Adusumilli, W.D. Travis, Three-dimensional histologic, immunohistochemical, and multiplex immunofluorescence analyses of dynamic vessel co-option of spread through air spaces in lung adenocarcinoma, J. Thorac. Oncol. 15 (2020) 589–600, https://doi.org/10.1016/j.jtho.2019.12.112.
[7] Y. Yu, D. Zeng, Q. Ou, S. Liu, A. Li, Y. Chen, D. Lin, Q. Gao, H. Zhou, W. Liao, H. Yao, Association of survival and immune-related biomarkers with immunotherapy in patients with non-small cell lung cancer: a meta-analysis and individual patient-level analysis, JAMA Netw. Open 2 (2019) e196879, https://doi.org/10.1001/jamanetworkopen.2019.6879.
[8] N.K. Altorki, A.C. Borczuk, S. Harrison, L.K. Groner, B. Bhinder, V. Mittal, O. Element, T.E. McGraw, Global evolution of the tumor microenvironment associated with progression from preinvasive invasive to invasive human lung adenocarcinoma, Cell Rep. 39 (2022) 110639, https://doi.org/10.1016/j.celrep.2022.110639.
[9] L. Zhang, Y. Chen, H. Wang, Z. Xu, Y. Wang, S. Li, J. Liu, Y. Chen, H. Luo, L. Wu, Y. Yang, H. Zhang, H. Peng, Massive PD-L1 and CD8 double positive TILs characterize an immunosuppressive microenvironment with high mutational burden in lung cancer, J. Immunother. Cancer 9 (2021) e002356, https://doi.org/10.1136/jitc-2021-002356.
[10] M. Backman, C. Strell, A. Lindberg, J.S.M. Mattsson, H. Elfving, H. Brunnström, A. O'Reilly, M. Bosic, M. Gulyas, J. Isaksson, J. Botling, K. Kärre, K. Jirström, K. Lamberg, F. Pontén, K. Leandersson, A. Mezheyeuski, P. Micke, Spatial immunophenotyping of the tumour microenvironment in non-small cell lung cancer, Eur. J. Cancer 185 (2023) 40–52, https://doi.org/10.1016/j.ejca.2023.02.012.